

# Development of Window Films for Solar Shading and Heat Insulating Applications

Tetsuya TAKEUCHI\*, Osamu GOTO, Masataka INUDUKA, Tetsuji NARASAKI, Yoshihiro TOKUNAGA, Hisami BESSHO and Hitoshi TAKEDA\*

Tokai Rubber Industries, Ltd. (TRI) has developed window films for solar shading and heat insulating applications by combining its advanced technologies of optical multi-layered membrane design, precision coating, and elongated sputtering, as well as material technology. The optical functional membrane is a multi-layered membrane that consists of thin Ag alloy membranes and thin dielectric membranes with a high refractive index. TRI has significantly reduced the cost of manufacturing the dielectric membranes by using its original sol-gel wet film forming method, and has accordingly succeeded in producing competitively-priced optical function membranes. The solar shading and heat insulating effects of the films were proven in the verification tests by using the experimental equipment of Tokyo University of Science. Furthermore, the energy-saving effects for annual air-conditioning-related power consumption were estimated by using the thermal load calculation program "LESCOM-wind" in a model office.

Keywords: window film, solar shading, heat insulating, infrared light, sol-gel

## 1. Introduction

In response to a growing awareness of energy-saving and power-saving and the need for improving the living environment near windows, the applications of transparent heat ray blocking films that can be affixed to window glass have been proposed.

We have promoted the development of optical functional films by combining our technologies of optical multi-layered membrane design, precision coating, and elongated sputtering, as well as material technology. We report here the development of transparent window films for solar shading and heat insulating applications which meet the market needs mentioned above very well.

## 2. Outline of the Development

### 2-1 Functions of the solar shading and heat insulating window films

As windows are required to ensure natural lighting and views, solar-shading and heat-insulating window films need to simultaneously pursue those goals while maintaining transparency. **Figure 1** shows the distribution of sunlight energy according to light wavelength, the distribution of warming radiant heat energy from indoors, the transmission and reflection spectrum that is required for window-affixed films to produce transparency, heat shielding (solar shading), and heat insulating functions. To enable windows to balance the maintenance of lighting and sunlight-energy-shielding, it is necessary to form cut-off filters that transmit visible light (wavelength: 0.4 to 0.8 $\mu\text{m}$ ) and reflect near-infrared light (wavelength: 0.8 to 2 $\mu\text{m}$ ) out of sunlight energy. Moreover, because the heat insulation functions are produced by reducing thermal discharge through the reflection of far-infrared light (wavelength 5 to 20 $\mu\text{m}$ ), which is warming radiant heat energy from indoors, to the indoor side, the reflection of far-infrared light is also required.

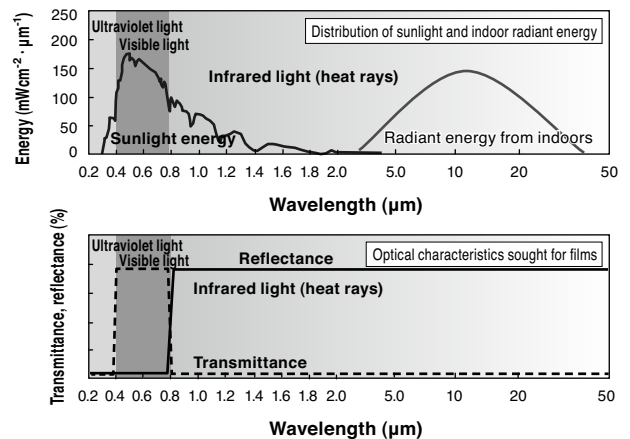


Fig. 1. Distribution of sunlight and indoor radiant heat energy, and optical characteristics sought for window-affixed films

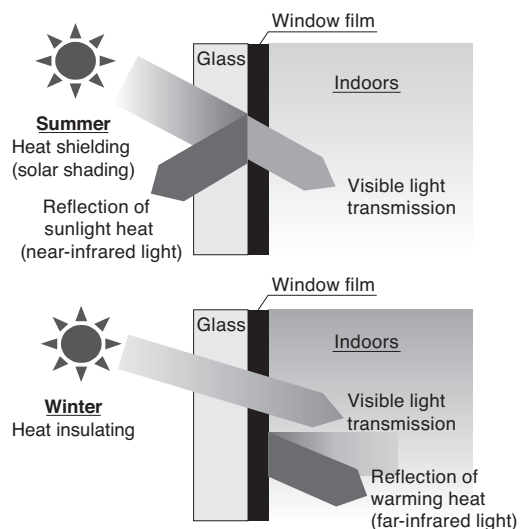


Fig. 2. Functions of solar shading and heat insulating films

Figure 2 shows the image of the functions of solar shading and heat insulating films in the summer and the winter.

## 2-2 Design and composition of functional membranes

When designing the functional membranes as optical multi-layered membrane filters, which can meet all demands for visible light transmission, near-infrared light reflection and far-infrared light reflection, we have selected Ag alloy membranes that absorb little visible light and largely reflect infrared light, as the layer possessing a low refractive index. Additionally, we have secured natural lighting and views by making the reflectance low and the transmittance high in the invisible light region through multi-layering of the alloy membranes and thin dielectric membranes possessing a high refractive index. According to the width of transparent wavelength in the required visible light region, starting inclination of the reflectance in the near-infrared light region and reflectance in the far-infrared light region, the number of layers made by thin dielectric membranes with high refractive index and Ag membranes, as well as the membrane thickness of each layer, are decided. Figure 3 shows the cross section photo of a seven-layered film.

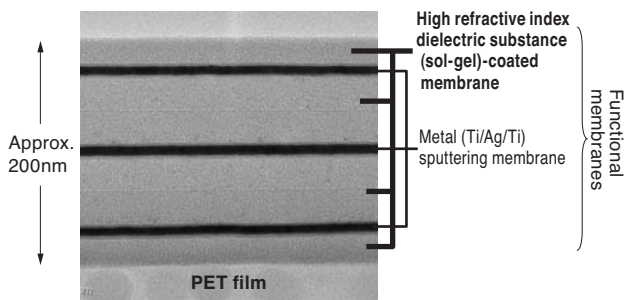


Fig. 3. Sectional structure (TEM image) of the functional membrane

The actual films are composed of thin dielectric membranes with high refractive index and Ag alloy membranes, alternately laminated on the PET film; several nm-thick Ti membranes are inserted into the interface between the thin dielectric membrane with high refractive index and the Ag membrane to limit Ag migration and enhance ply adhesion.

## 2-3 Technology of adding heat insulating functions

To add heat insulating functions, it is necessary to reflect warming heat (far-infrared light) generated from indoors to the indoor side without absorbing it. Conventional solar shading films, however, have no heat insulating functions because the PET film and acrylic hard coating are placed on the indoor side of functional membranes (heat ray reflective coating), and the films in that combination absorb warming heat (far-infrared light). Therefore, we have simultaneously pursued heat insulating properties and abrasion resistance by changing the film composition from the glass side to the order of the adhesive layer, PET film, heat ray reflection function membranes, acrylic protective membranes and acrylic hard coating and by controlling the

thickness of hard coating membranes and protective membranes respectively to the appropriate range of not more than 1  $\mu\text{m}$ . Figure 4 shows the film compositions of the solar shading and heat insulating type and the solar shading type.

	Film composition (cross section)	Function	
		Solar shading	Heat insulating
Solar shading and heat insulating type		○	○
Solar shading type		○	×

Fig. 4. Structure of the solar shading and heat insulating films

## 2-4 Functional membranes manufacturing technology

We have significantly reduced the cost of manufacturing thin dielectric membranes with a high refractive index, which are one component of functional membranes, by using the wet coating method that ensures high linear speed in the air, instead of high-cost reactive sputtering film formation. Made by using organic titanate as the material, the membranes are coated by the gravure roll method, and, after being dried, they are subjected to a low-temperature sol-gel polymerization reaction by UV irradiation, which makes the formation of titanium dioxide ( $\text{TiO}_2$ ) on the PET film possible. Considering stability in coating fluid, the ease of producing a high refractive index and the unlikelihood of generating cracks, we have used n-butoxytitanium (multimer) for organic titanate, which is chelated by acetylacetone to add UV absorbency. Figure 5 shows the mechanism of the UV assist sol-gel polymerization reaction.

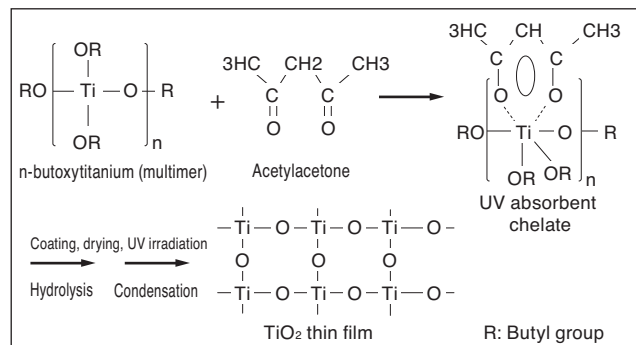


Fig. 5. Mechanism of UV assist sol-gel polymerization reaction

### 3. Characteristics of the Solar Shading and Heat Insulating Films

#### 3-1 Optical characteristics

We have developed three types of window films for solar shading and heating insulating applications: “Refle-shine TX71” with solar shading functions, “Refle-shine TW31” with heat insulating functions, and “Refle-shine TU71” with solar shading and heat insulating functions. **Figures 6 to 8** show the transmission and reflection spectrum in the ultraviolet to the far-infrared light region. Each figure, respectively, shows that the solar shading film “Refle-shine TX71” has visible light transmission and near-infrared light reflection functions; that the heat insulating film “Refle-shine TW31” has visible light transmission and far-infrared light reflection functions; and that the solar shading and heat insulating film “Refle-shine TU71” has

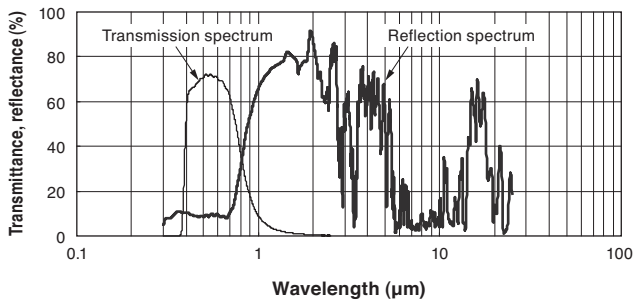


Fig. 6. Transmission and reflection spectrum of the solar shading film “Refle-shine TX71”

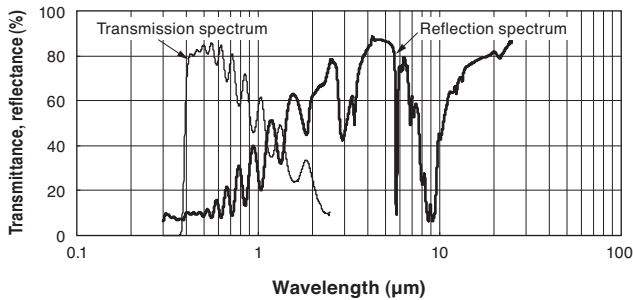


Fig. 7. Transmission and reflection spectrum of the heat insulating film “Refle-shine TW31”

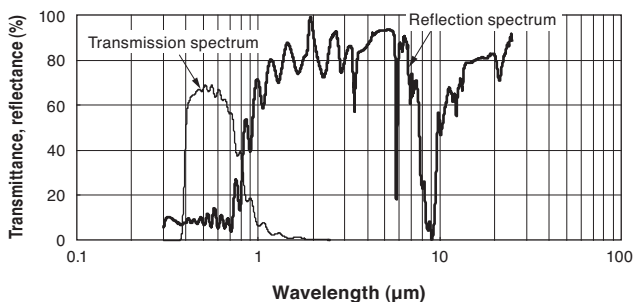


Fig. 8. Transmission and reflection spectrum of the solar shading and heat insulating film “Refle-shine TU71”

visible light transmission and near-infrared light to far-infrared light reflection functions.

**Table 1** shows the characteristics of “Refle-shine TX71”, “Refle-shine TW31” and “Refle-shine TU71”. The three types of film ensure good lighting with more than 70% of visible light transmittance. TX71 and TU71 ensure high solar shading with a shading coefficient of not higher than 0.6. Also, TW31 and TU71 ensure good heat insulation with the overall heat transfer coefficient of not more than 4.5 W/m<sup>2</sup>K. In particular, TU71 is the world's first film that ensures transparency, solar shading and heat insulating characteristics.

**Table 1.** Characteristics of “Refle-shine TX71”, “Refle-shine TW31” and “Refle-shine TU71”

		Solar shading type	Heat insulating type	Solar shading and heat insulating type	Reference
		Refle-shine TX71	Refle-shine TW31	Refle-shine TU71	Only 3mm-thick plate glass
Lighting	Visible light transmittance	71.0%	81.6%	70.8%	90.4%
	Shading coefficient	0.57	0.74	0.51	1.00
Solar shading	Solar transmittance	39.6%	61.0%	37.0%	87.4%
	Overall heat transfer coefficient	5.77W/m <sup>2</sup> K	4.49W/m <sup>2</sup> K	4.47W/m <sup>2</sup> K	5.92W/m <sup>2</sup> K
Safety of glass against heat cracking	Solar absorptance	32.4%	19.0%	34.1%	4.4%

Test method: Measured by affixing the films to 3mm-thick plate glass, based on JISA5759 “Films for building window glass”

#### 3-2 Weather resistance

Based on JISA5759 “Films for building window glass,” films for building windows should be subjected to the weather

**Table 2.** Weather resistant test conditions

Item	Condition
Light source	Sunshine carbon-arc lamp: 1 unit
	Light filter
	Spectral transmittance Not more than 2% at 275nm Not less than 90% at 400nm
Power supply voltage	AC 200V±20V
Conditions for irradiation	
Mean discharge voltage of power source	50V±1V, 60A±1.2A
Temperature indicated by black panel thermometer	63°C±3°C
Relative humidity	(50±5)%
Irradiance on the surface of specimen	255 (±10%) W/m <sup>2</sup> (at 300nm to 700nm)
Water jetting	Normally, water is jetted for 18 minutes during 120 minutes of irradiation.
Film-affixed glass	Spectral transmittance Not more than 2% at 275nm Not less than 90% at 400nm
Conditions of photoirradiation to specimen	Affixed with the glass surface facing the light source.
Method of water jetting	Water is jetted to the glass surface on the photo-irradiation side.

**Table 3.** Comparison of the characteristics of “Refle-shine TX71,” “Refle-shine TW31” and “Refle-shine TU71” before and after the test

Type	Item	Initial stage	After weather resistant test
Solar shading type TX71	Visible light transmittance	71.0%	71.8%
	Shading coefficient	0.57	0.56
	Solar transmittance	39.6%	39.2%
	Overall heat transfer coefficient	5.77W/m <sup>2</sup> K	5.79W/m <sup>2</sup> K
	Solar absorptance	32.4%	31.8%
Heat insulating type TW31	Visible light transmittance	81.6%	79.4%
	Shading coefficient	0.74	0.74
	Solar transmittance	61.0%	60.0%
	Overall heat transfer coefficient	4.49W/m <sup>2</sup> K	4.63W/m <sup>2</sup> K
	Solar absorptance	19.0%	20.4%
Solar shading and heat insulating type TU71	Visible light transmittance	70.8%	71.6%
	Shading coefficient	0.51	0.54
	Solar transmittance	37.0%	37.8%
	Overall heat transfer coefficient	4.47W/m <sup>2</sup> K	4.52W/m <sup>2</sup> K
	Solar absorptance	34.1%	30.4%

resistant test by using a weatherometer of the sunshine carbon-arc lamp type. **Table 2** shows the test conditions.

**Table 3** shows the test results of “Refle-shine TX71,” “Refle-shine TW31” and “Refle-shine TU71.” The results confirmed that there were no changes in appearance and optical characteristics of the three films after 1,000 hours had passed since the start of the test.

#### 4. Experimental Verification of the Solar Shading and Heat Insulating Effects

##### 4-1 Experimental methodology

We have verified the thermal effects of the developed solar shading and heat insulating films by using the experimental equipment of Tokyo University of Science. **Photo 1** shows the experimental equipment.

There are six units of experimental equipment (hereinafter referred to as “test box”), of which four units were



**Photo 1.** Experimental equipment

used. The test box has an opening, 1 m wide and 2 m high on the southern side, to which single plate glass or multiple-layer glass is installed. Heat insulation is applied by polystyrene foam, 100 mm thick, to all parts of the test boxes, except the glass surface. Among the four test boxes, solar shading and heat insulating films were affixed to the inside of the glass for three units, while the remaining unit was left with nothing affixed to the glass for comparison. Using a PC and data logger, we performed the experiments by measuring the air temperature in the test boxes, temperature inside the glass, and the amount of transmitted solar radiation at intervals of one minute for 24 consecutive hours. **Figure 9** shows the installation of sensors in the test boxes. When measuring heat insulating effects, 400 W far-infrared ray heaters were installed, facing the polystyrene foam side opposite the glass surface in each test box and the on/off control of the heaters was simultaneously performed in the all test boxes, to maintain a temperature between 20°C and 25°C with the air temperature at a height of 150 cm from the floor, within the glass-only test box as the standard<sup>(1), (2)</sup>.

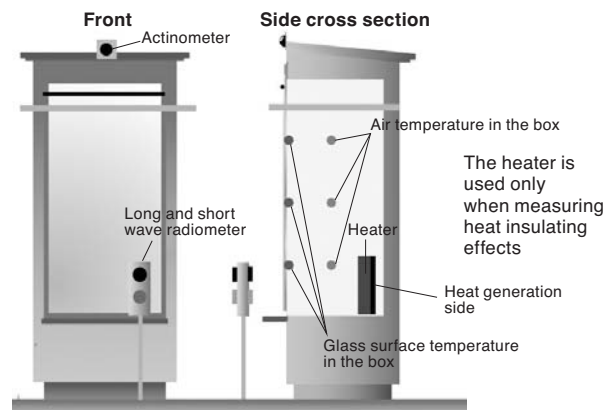


**Fig. 9.** Installation of sensors in the test box

Regarding solar shading and heat insulating effects, using single plate glass or multiple-layer glass for the opening of the test box, the comparison was made respectively between the situation of affixing solar shading and heat insulating films to the glass and a control setup using glass

**Table 4.** List of experiments performed

	Used glass	Season	Test date
Verification of solar shading effects	Single plate glass 8mm thick	Winter to interim period	February 3 to 20, 2011
		Summer	June 28 to July 31, 2011
	Multiple-layer glass 8/A6/8mm	Winter to interim period	April 2 to 30, 2011
		Summer	June 1 to 26, 2011
Verification of heat insulating effects	Single plate glass 8mm thick	Winter to interim period	March 14 to 15, 2011
		Summer	—
	Multiple-layer glass 8/A6/8mm	Winter to interim period	April 7 to 8, 2011
		Summer	—

only. The experiments were performed from the winter through the interim period and in the summer. **Table 4** shows the list of experiments performed.

#### 4-2 Experimental results

##### (1) Verification of solar shading effects

###### (a) When affixed to single plate glass

**Figure 10** shows the temporal fluctuation of air temperature in the box when the films were affixed to the inside of the 8mm-thick single plate glass. They are the results on February 5 to 7, 2011 in the winter and the interim period, and the results on July 12 to 14, 2011 in the summer. When the experiments were performed, meteorological data were also simultaneously measured. As an example, **Fig. 11** shows the data of outdoor air temperature and vertical intensity of solar radiation in the winter and the interim period and the summer experimental period.

In the measurements made in the winter and the interim period, February 5 and 6 were cloudy and on February 7 there was fine weather. In the measurements made in the summer, July 12 and 13 were cloudy and on July 14 there was fine weather. When there was sunlight, the air temperature in the box fell by up to 12.9°C for TU71, 11.9°C for TX71 and 4.8°C for TW31 in the winter and 3.9°C for TU71, 4.1°C for TX71, and 0.6°C for TW31 in the summer, compared with the box with only glass installed with no films. It is confirmed from the results that there were temperature rise restraining effects when the films were affixed to the glass and that the smaller the shading coefficient was, the larger the temperature rise restraining effects were.

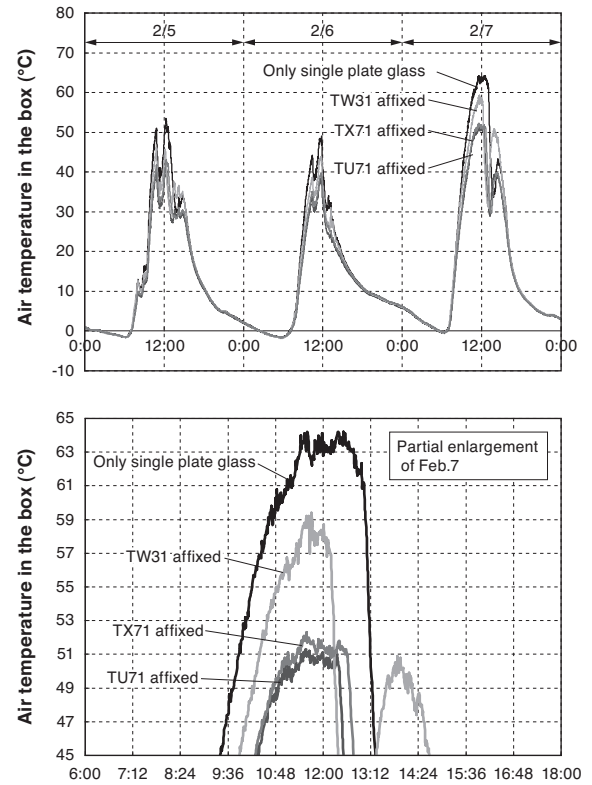
In addition, the rising of air temperature in the box was lower in the summer than in the winter. This is because the vertical intensity of solar radiation on the southern side, where the opening was installed, is smaller in the summer, which decreases the amount of solar radiation flowing into the box.

###### (b) When affixed to multiple-layer glass

**Figure 12** shows the temporal fluctuation of air temperature in the box when TU71 was affixed to the inside of the multiple-layer glass [glass 8 mm / air 6 mm / glass 8 mm]. The measurement in the case when the LowE multiple-layer glass of the same thickness (shading coefficient 0.69, overall heat transfer coefficient 2.5 W/m<sup>2</sup>K) was used was simultaneously made for comparison. These are the results from April 14 to 16, 2011, in the winter and the interim period and the results from June 5 to 7, 2011, in the summer. In the measurements made in the winter and the interim period, on April 14 and 15 there was fine weather and April 16 was cloudy. In the measurements made in the summer, June 5 and 7 were cloudy and on June 6 there was fine weather.

The air temperature in the box fell by up to 7.4°C for TU71 and 4.3°C for the LowE multiple-layer glass in the winter and the interim period and 2.9°C for TU71 and 1.2°C for the LowE multiple-layer glass in the summer, compared with the box where only multiple-layer glass was installed with no films. From the above-mentioned results, even in the case of multiple-layer glass, it is confirmed that there were temperature rise restraining effects when the films were affixed to the glass and that, the smaller the shading coefficient was, the larger the temperature rise re-

##### (1) Experiments in the winter to the interim period



##### (2) Experiments in the summer

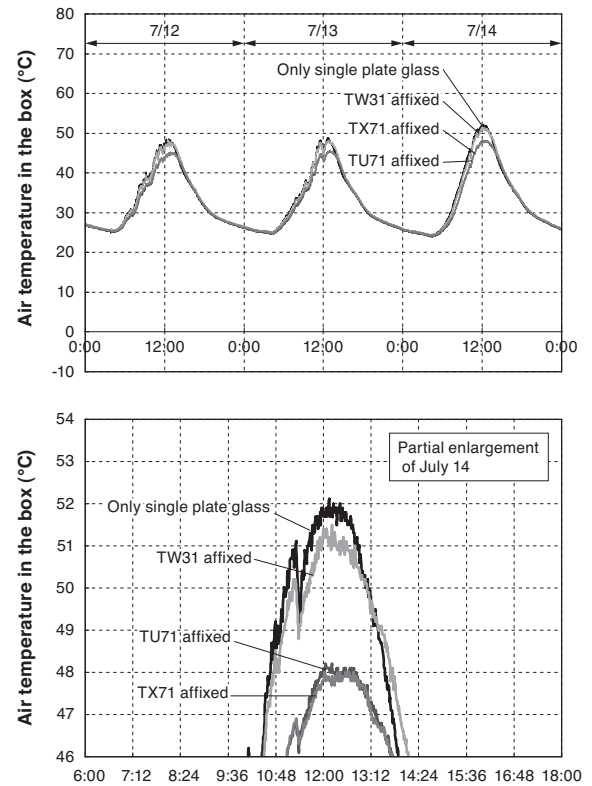
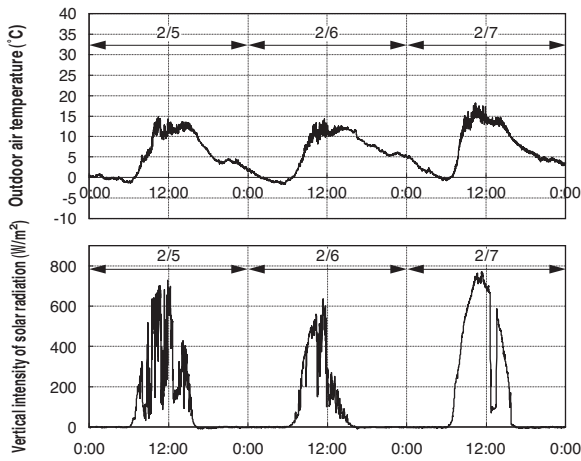


**Fig. 10.** Temporal fluctuation of air temperature in the box in (1) the experiments in the winter to the interim period and (2) the experiments in the summer (in the case of single plate glass)

(1) Meteorological data of the experiments in the winter to the interim period



(2) Meteorological data of the experiments in the summer

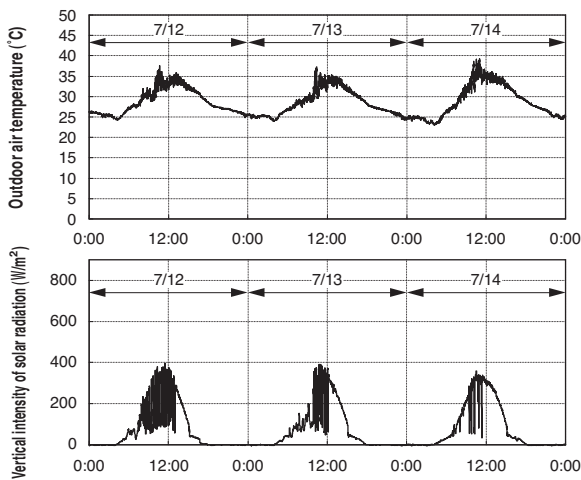
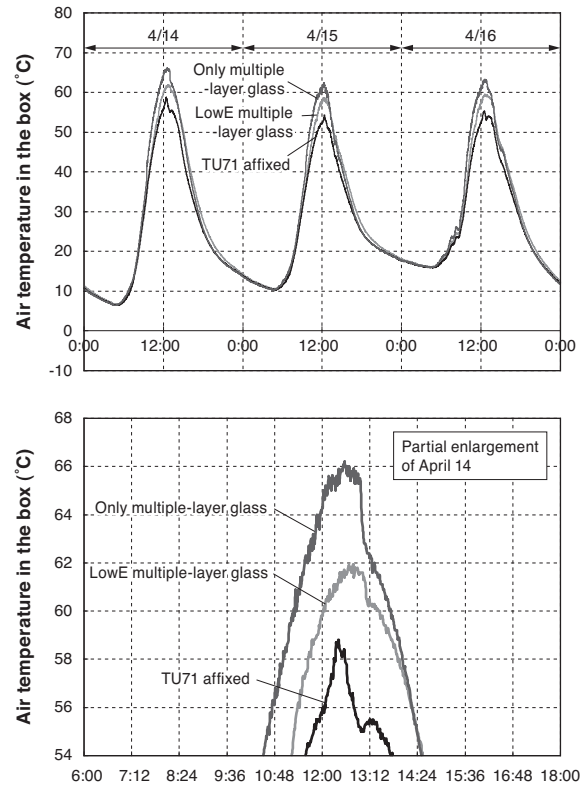


Fig. 11. Examples of the meteorological data during the experimental periods

(1) Experiments in the winter to the interim period



(2) Experiments in the summer

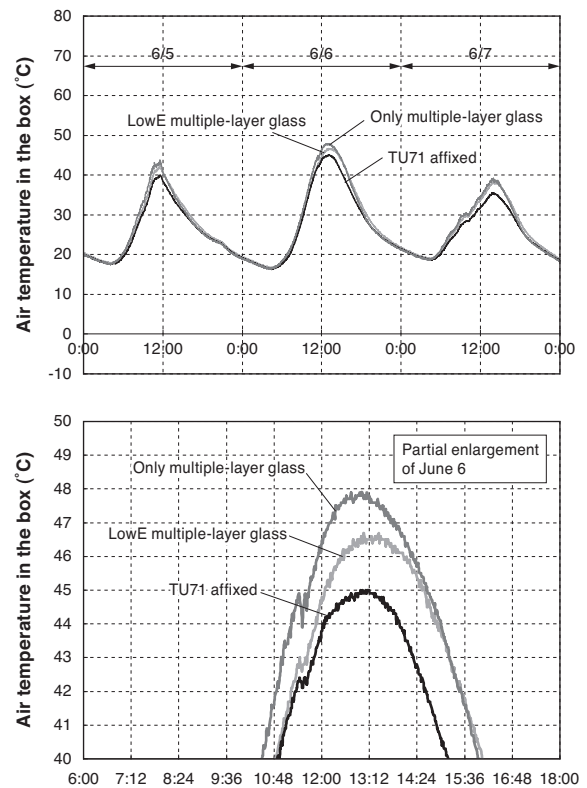


Fig. 12. (1) Temporal fluctuation of air temperature in the box in (1) the experiments in the winter to the interim period and (2) the experiments in the summer (in the case of multiple-layer glass)

straining effects were.

(2) Verification of heat insulating effects  
(a) When affixed to the single plate glass

The experiments in the cases where the heat insulating type TW31 and the solar shading type TX71 were affixed to the inside of the 8mm-thick single plate glass, were performed between March 14 and 15, 2011. The experiments were performed at night to avoid the effects of heat from sunlight. **Figure 13** shows the temporal fluctuation of the air temperature in the box. Moreover, **Fig. 14** shows the data of outdoor air temperature and the vertical intensity of solar radiation during the experimental period.

400 W far-infrared ray heaters were installed in each test box and the on/off control of the heaters was simultaneously performed in the all test boxes, to maintain a temperature between 20°C and 25°C with the air temperature at a height of 150 cm from the floor within the glass-only test box as the standard. The air temperature in the box repeats in a rising and falling waveform. When the heat insulating type TW31 was affixed to the glass, the temperature

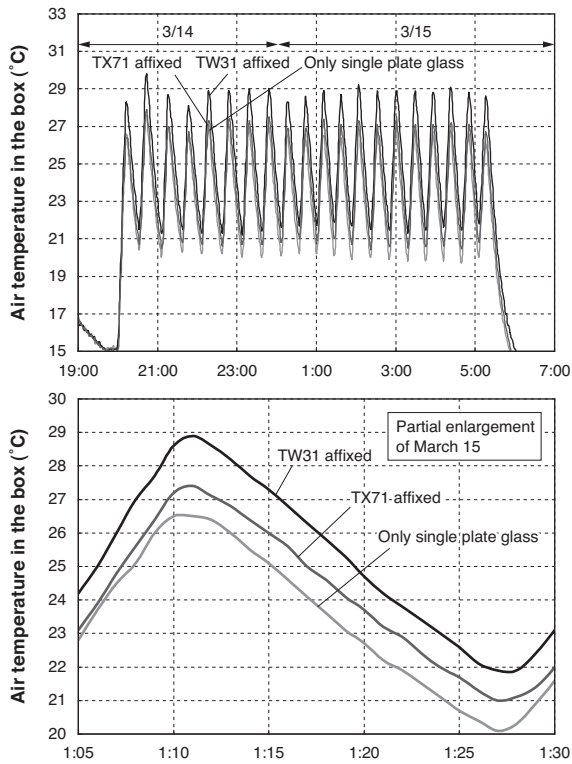


Fig. 13. Temporal fluctuation of air temperature in the box (in the case of single plate glass)

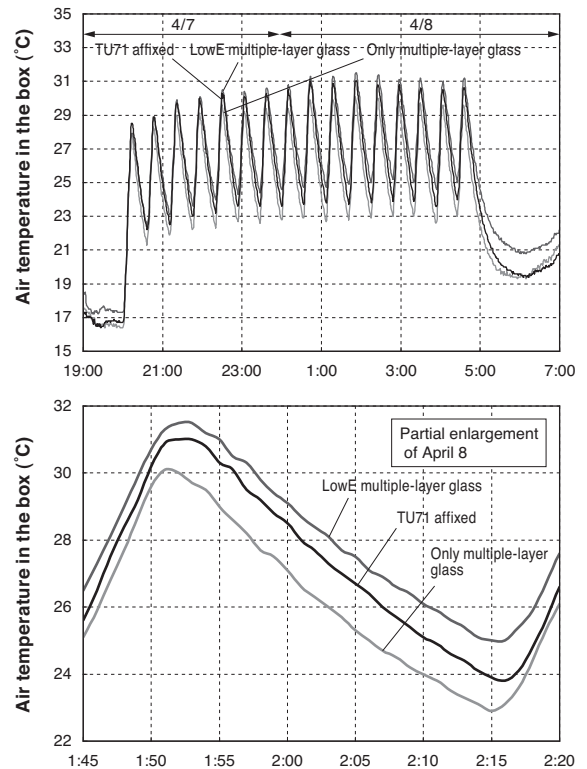


Fig. 15. Temporal fluctuation of the air temperature in the box (in the case of multiple-layer glass)

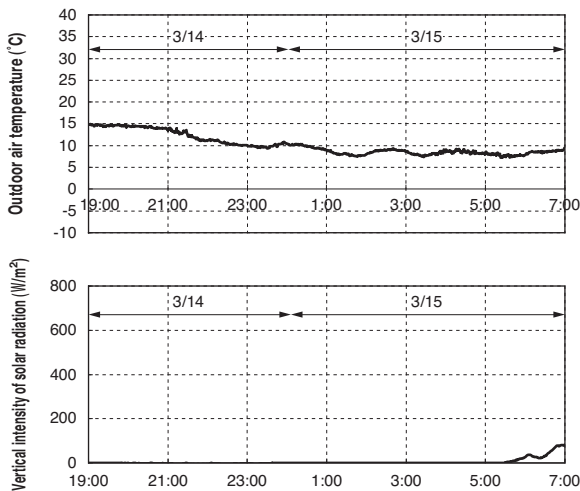


Fig. 14. Example of the meteorological data during the experimental period

increased up to 2.7°C compared with the box with only glass installed with no films, and the heat insulating effects were confirmed. Moreover, when the solar shading type TX71 was affixed to the glass, the temperature increased 1.1°C.

(b) When affixed to the multiple-layer glass

The experiments in the cases where the solar shading and heat insulating type TU71 was affixed to the inside of the multiple-layer glass [glass 8 mm/ air 6 mm/ glass 8 mm] were performed from April 7 to 8, 2011. The meas-

urement in the case where the LowE multiple-layer glass of the same thickness (shading coefficient 0.69, overall heat transfer coefficient 2.5 W/m<sup>2</sup>K) was used was simultaneously made for comparison. The tests were performed at night to avoid the effects of heat from sunlight. Figure 15 shows the temporal fluctuation of the air temperature in the boxes.

When the solar shading and heat insulating type TU71 was affixed to the glass, the temperature increased up to 1.0°C, compared with the box with only multiple-layer glass installed with no films and the heat insulating effects were confirmed. Moreover, when the LowE multiple-layer glass was used, the temperature increased 1.5°C.

(3) Summary of the results

The experimental results mentioned above are summarized in Table 5.

## 5. Simulation Verification of Solar Shading and Heat Insulating Effects

### 5-1 Simulation method

We have verified the thermal effects of the solar shading and heat insulating films we have developed, this time using the non-stationary thermal-load calculation program “LESCOM-wind” based on the response factor method. “LESCOM-wind” was developed for the parameters appropriate for the calculation of the effectiveness of window films intended for solar shading and heating insulating ap-

**Table 5.** Summary of the solar shading and heat insulation effects verification experiments

	Used glass	Season	Effects of affixing the films (Comparison of the difference of air temperature in the boxes compared with the box with only glass installed with no films)				Reference
			Standard	Solar shading film (TX71) affixed	Heat insulating film (TW31) affixed	Solar shading and heat insulating film (TU71) affixed	LowE multiple-layer glass
Verification of solar shading effects	Single plate glass 8mm thick	Winter to interim period	Based on the case of only single plate glass	11.9°C down	4.8°C down	12.9°C down	
		Summer		4.1°C down	0.6°C down	3.9°C down	
	Multiple-layer glass 8/A6/8mm	Winter to interim period	Based on the case of only multiple-layer glass	—	—	7.4°C down	4.3°C down
		Summer		—	—	2.9°C down	1.2°C down
Verification of heat insulating effects	Single plate glass 8mm thick	Winter to interim period	Based on the case of only single plate glass	1.1°C up	2.7°C up	—	
		Summer					
	Multiple-layer glass 8/A6/8mm	Winter to interim period	Based on the case of only multiple-layer glass	—	—	1.0°C up	1.5°C up
		Summer					

plications, based on the multi-room non-stationary thermal load calculation program “LESCOM,” developed by the task force for “living function enhancement products” of the former Ministry of International Trade and Industry, Consumer Goods Industries Bureau<sup>(3)-(6)</sup>.

**Figure 16** shows the conceptual diagram of heat balance of the opening, which is extremely complicated and wide-ranging. The non-stationary thermal load calculation program “LESCOM-wind” reproduces the thermal environment by computer simulation, based on a thermal equilibrium formula in consideration of such heat balance.

**5-2 Results of simulation verification**

(1) Verification of solar shading effects

We have verified the solar shading effects by performing the simulation calculation, namely; the thermal load calculation based on the actual test box experiments, using the thermal load calculation program “LESCOM-wind.” The calculation was performed based on the solar shading experiments using the 8 mm-thick single plate glass, which were performed from February 5 to 7, 2011, by using the meteorological data of the relevant days. **Figure 17** shows the simulation calculation results and the actual measurement data of the air temperatures in the box when TX71 was affixed to the glass. The simulation calculation results using “LESCOM-wind” conformed to the actual measurement data very well and the solar shading effects of TX71 were also confirmed by the simulation calculation.

(2) Verification of heat insulating effects

As in the case of (1), using the thermal load calculation program “LESCOM-wind,” the simulation calculation was performed based on the heat insulating experiments conducted on March 14 and 15, 2011, using the 8 mm-thick single plate glass and the meteorological data of the relevant days. **Figure 18** shows the simulation calculation results and the actual measurement data of the air temperatures in the box when TW31 was affixed to the glass. The

simulation calculation results using “LESCOM-wind” conformed to the actual measurement data very well, and the heat insulating effects of TW31 were also confirmed by the simulation calculation.

**6. Air-Conditioning Load Simulation in a Model Office**

**6-1 Simulation method**

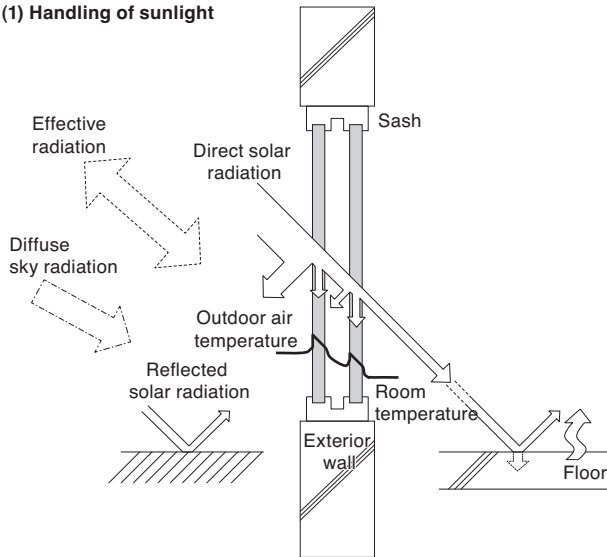
As it was confirmed that the calculation results conformed well to the experimental results in the test boxes, using the thermal load calculation program “LESCOM-wind,” we have performed the simulation calculation of energy-saving effects for annual air-conditioning-related power consumption in the case where solar shading and heat insulating films were used in a model office designated by the Architectural Institute of Japan. The calculations were performed in three locations—Sapporo, Tokyo, and Naha. **Table 6** shows the simulation calculation conditions, while **Fig. 19** shows the plan view of a model office designated by the Architectural Institute of Japan<sup>(7)</sup>.

**6-2 Simulation results**

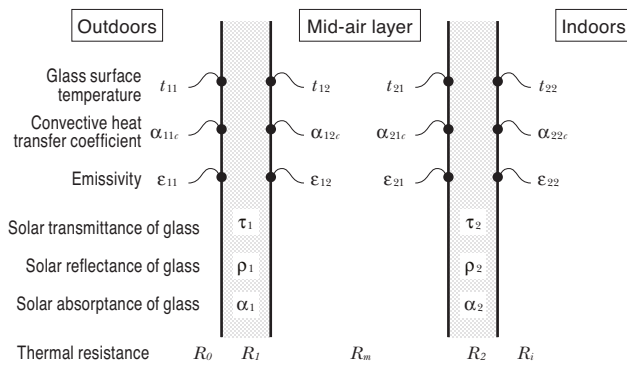
**Figure 20** shows the annual air-conditioning-related power consumption when TU71, TW31, and TX71 were respectively affixed to the 8 mm-thick single plate glass. **Figure 21** shows the annual air-conditioning-related power consumption when TU71 was affixed to the multiple-layer glass [glass 8 mm / air 6 mm / glass 8 mm]. **Table 7** shows the annual air-conditioning-related thermal load in Tokyo when the films were affixed to the single plate glass. **Table 8** shows the annual air-conditioning-related thermal load in Tokyo when the films were affixed to the multiple-layer glass. **Figure 21** and **Table 8** show the calculation results when the LowE multiple-layer glass of the same thickness



**(1) Handling of sunlight**



**(2) Heat balance**



- $t_{11}$  : Outdoor glass external surface temperature [°C]
- $t_{12}$  : Outdoor glass inner surface temperature [°C]
- $t_{21}$  : Indoor glass external surface temperature [°C]
- $t_{22}$  : Indoor glass inner surface temperature [°C]
- $t_m$  : Mid-air layer temperature [°C]
- $\alpha_{11c}$  : Outdoor glass external surface convective heat transfer coefficient [W/m<sup>2</sup>·K]
- $\alpha_{11r}$  : Outdoor glass external surface radiative heat transfer coefficient [W/m<sup>2</sup>·K]
- $\alpha_{12c}$  : Outdoor glass inner surface convective heat transfer coefficient [W/m<sup>2</sup>·K]
- $\alpha_{21c}$  : Indoor glass external surface convective heat transfer coefficient [W/m<sup>2</sup>·K]
- $\alpha_{22c}$  : Indoor glass inner surface convective heat transfer coefficient [W/m<sup>2</sup>·K]
- $\alpha_{22r}$  : Indoor glass inner surface radiative heat transfer coefficient [W/m<sup>2</sup>·K]
- $\epsilon_{11}$  : Outdoor glass external surface emissivity [—]
- $\epsilon_{12}$  : Outdoor glass inner surface emissivity [—]
- $\epsilon_{21}$  : Indoor glass external surface emissivity [—]
- $\epsilon_{22}$  : Indoor glass inner surface emissivity [—]
- $R_0$  : Outdoor heat transfer resistance [m<sup>2</sup>·K/W]
- $R_1$  : Outdoor glass thermal resistance (constant) [m<sup>2</sup>·K/W]
- $R_m$  : Mid-air layer heat transfer resistance [m<sup>2</sup>·K/W]
- $R_2$  : Indoor glass thermal resistance (constant) [m<sup>2</sup>·K/W]
- $R_i$  : Indoor heat transfer resistance [m<sup>2</sup>·K/W]
- $R$  : Total thermal resistance of the glass part [m<sup>2</sup>·K/W]

**Fig. 16.** Conceptual diagram of heat balance of the opening (in the case of multiple-layer glass)

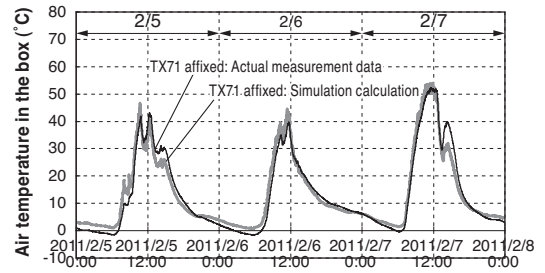


**Fig. 17.** Comparison of the simulation calculation results and the actual measured values when TX71 was affixed to the glass

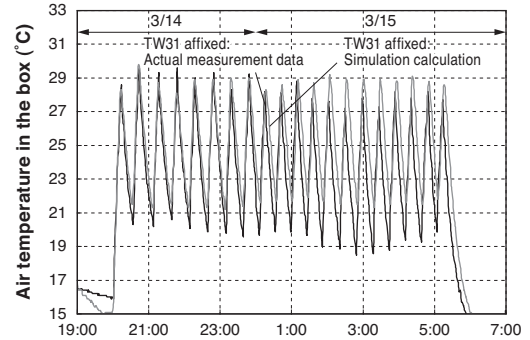


**Fig. 18.** Comparison of the simulation calculation results and the actual measured values, when TW31 was affixed to the glass

**Table 6.** Simulation calculation conditions

item	Calculation conditions
Calculation program	“LESCOM-wind”
Calculation point	Sapporo, Tokyo, Naha
Meteorological data	Using the typical annual data in the 1990s
Building model	One floor of an office model designated by the Architectural Institute of Japan Target floor area: 605m <sup>2</sup> (office part) Window area: 150m <sup>2</sup>
Glass type	8mm-thick single plate glass or 8/A6/8mm multiple-layer glass with the solar shading and heat insulating films affixed (to the room sides of all windows)
Air-conditioning setting	Cooling preset temperature: 26.7°C, Heating preset temperature: 21.9°C Air conditioning operating time: 8:00 to 18:00

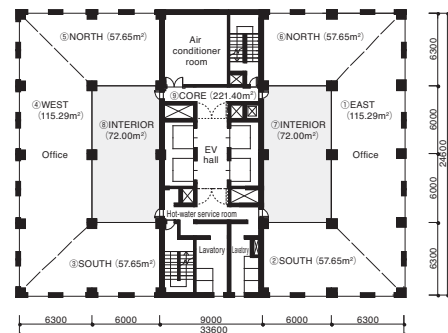


**Fig. 19.** Plan view of an office model designated by the Architectural Institute of Japan

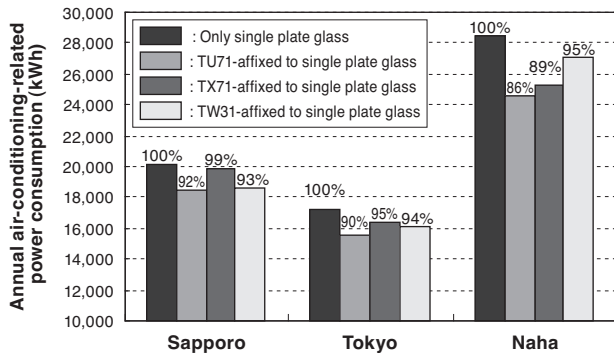


Fig. 20. Calculation results when the films were affixed to the single plate glass

Table 7. Calculation results for the annual air-conditioning-related thermal load in Tokyo when the films were affixed to the single plate glass

	Annual cooling and heating load		Annual cooling load kWh/ year	Annual heating load kWh/ year
	kWh/ year	Relative ratio		
Only single plate glass	17,198	100%	13,028	4,170
TU71-affixed to single plate glass	15,502	90%	11,017	4,485
TX71-affixed to single plate glass	16,332	95%	11,266	5,067
TW31-affixed to single plate glass	16,136	94%	12,360	3,775

The relative ratio shows the rate when the air-conditioning-related thermal load in using the single plate glass was regarded as 100.

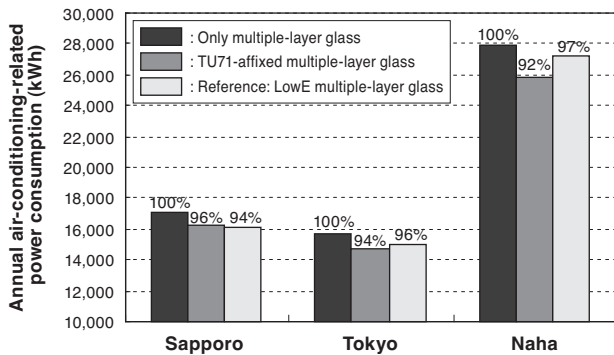


Fig. 21. Calculation results when the films were affixed to the multiple-layer glass

Table 8. Calculation results for the annual air-conditioning-related thermal load in Tokyo when the films were affixed to the multiple-layer glass

	Annual cooling and heating load		Annual cooling load kWh/ year	Annual heating load kWh/ year
	kWh/ year	Relative ratio		
Only multiple-layer glass	15,668	100%	13,056	2,612
TU71-affixed multiple-layer glass	14,726	94%	11,835	2,892
Reference: LowE multiple-layer glass	15,004	96%	12,711	2,293

The relative ratio shows the rate when the air-conditioning-related thermal load in using the multiple-layer glass was regarded as 100.

(shading coefficient 0.69, overall heat transfer coefficient  $2.5 \text{ W/m}^2\text{K}$ ) was used, for comparison. The comparison of the results for the single plate glass shows that, in all locations — Sapporo, Tokyo, and Naha — affixing the solar shading and heat insulating films to the glass had the effects of reducing the annual air-conditioning-related power consumption, compared with the conditions where no films were used. In particular, it is confirmed that TU71, which has both solar shading and heat insulating functions, had the largest reduction effects in all the locations. Moreover, it is confirmed from the simulation results that affixing TU71 to the multiple-layer glass had the reduction results equivalent to those of the LowE multiple-layer glass (shading coefficient 0.69, overall heat transfer coefficient  $2.5 \text{ W/m}^2\text{K}$ ).

## 7. Conclusion

We have developed window films for solar shading, heat insulating, and solar shading and heat insulating by combining our technologies of optical multi-layered membrane design, precision coating, and elongated sputtering, as well as making advances in material technology. The optical functional membranes consist of membranes alternately laminated with the Ag alloy membrane and dielectric membranes with a high refractive index. In particular, we have significantly reduced the cost of forming dielectric membranes with a high refractive index based on our original sol-gel wet film formation method. Through verification using the experimental equipment of Tokyo University of Science and the simulation verification using the thermal load calculation program “LESCOM-wind,” we have clarified the solar shading and heat insulating effects of our films. Moreover, we have calculated the energy-saving effects for annual air-conditioning-related power consumption in a model office.

In the future, we aim to develop constituent materials and make the design of functional membranes more widely applicable and are planning to achieve even higher performance and greater cost reductions for the films.

### Technical Term

- \*1 Shading coefficient: The numerical value that expresses the heat quantity of sunlight energy inflow, when the indoor inflow heat quantity by the transmission through, and reradiation from, a 3 mm-thick transparent plate glass is 1.00
- \*2 Overall heat transfer coefficient: The numerical value that expresses the heat quantity passing the area of 1 m<sup>2</sup> per hour when there is a temperature difference of 1°C.
- \*3 Glass heat cracking: When a sheet of window glass receives direct sunlight, the parts exposed to sunlight warm and expand, but the surrounding parts below the sash and shaded parts warm only slightly and remain at a comparatively low temperature. This low-temperature part restrains the expansion of warmed parts and, as a result, tensile stress occurs in the surrounding glass edge. When the stress exceeds edge strength of the glass, "heat cracking of the glass" occurs.
- \*4 Cooling load: The amount of energy required for cooling a room to a certain temperature.
- \*5 Heating load: The amount of energy required for warming a room to a certain temperature.

### References

- (1) Tetsuya Takeuchi, Hitoshi Takeda, Hiroki Inagaki, Hisami Bessho: The study concerning solar shading and heat insulating effects of the solar shading films, Part 1, Experimental verification of solar shading effects, Digest of academic lectures of the Architectural Institute of Japan, D-2, pp563-564, 2011
- (2) Hiroki Inagaki, Hitoshi Takeda, Tetsuya Takeuchi, Hisami Bessho: The study concerning solar shading and heat insulating effects of solar shading films, Part 2, Experimental verification of the heat insulating effects of low radiation films, Digest of academic lectures of the Architectural Institute of Japan, D-2, pp565-566, 2011
- (3) Yo Matsuo, Hitoshi Takeda: The thermal load calculation method based on the response factor method and the sample calculation (1), The journal of the Society of Heating, Air-Conditioning and Sanitary Engineers of Japan, Vol.44 No.4, pp1-14, 1970
- (4) Yo Matsuo, Hitoshi Takeda: The thermal load calculation method based on the response factor method and the sample calculation (2), The journal of the Society of Heating, Air-Conditioning and Sanitary Engineers of Japan, Vol. 44 No.7, pp11-25, 1970
- (5) Hitoshi Takeda: Room temperature fluctuation analysis for non-air-conditioned rooms, the collection of papers of the Society of Heating, Air-Conditioning and Sanitary Engineers of Japan, No. 7, pp13-21, 1978
- (6) Hitoshi Takeda, Minoru Inanuma, Nozomu Yoshizawa, Kyoichiro Isozaki: Standard meteorological data and thermal load calculation program, LESCO, Inoueshoin, 2005
- (7) Hiroshi Takizawa: Proposal of typical problems - Typical problems for office, Architectural Institute of Japan, Research Committee on Environmental Engineering, Documents of the 15th Heat Symposium, pp35-42, 1985

\* Refle-shine is a trademark or registered trademark of Tokai Rubber Industries, Ltd.

### Contributors (The lead author is indicated by an asterisk (\*).)

#### T. TAKEUCHI\*

- Project Deputy General Manager, New Business R&D Laboratories, Tokai Rubber Industries, Ltd.  
Engaged in the development of optical functional films



#### O. GOTO

- New Business R&D Laboratories, Tokai Rubber Industries, Ltd.

#### M. INUDUKA

- New Business R&D Laboratories, Tokai Rubber Industries, Ltd.

#### T. NARASAKI

- Project Manager, New Business R&D Laboratories, Tokai Rubber Industries, Ltd.

#### Y. TOKUNAGA

- Deputy Manager, Refle-shine Functional Film Business Unit, Tokai Rubber Industries, Ltd.

#### H. BESSHO

- General Manager, New Business R&D Laboratories, Tokai Rubber Industries, Ltd.

#### H. TAKEDA\*

- Doctor of Engineering  
Professor Emeritus, Tokyo University of Science, Specializes in environmental engineering of architecture

